

APPLICATION OF THE TRANSPIRATION METHOD FOR AEROSERVOELASTIC PREDICTION USING CFD

Cole H. Stephens* and Andrew S. Arena, Jr.†
 Oklahoma State University
 School of Mechanical and Aerospace Engineering
 Stillwater, OK
 and
 Kajal K. Gupta‡
 NASA Dryden Flight Research Center
 Edwards, CA

Abstract

Research presented in this paper illustrates the implementation of the transpiration boundary condition in steady and unsteady aeroelastic and aeroservoelastic simulations. For two reference cases, the AGARD 445.6 wing and the BACT wing with a finite-span flap, application of the transpiration method has demonstrated the effectiveness of applying the transpiration boundary condition at a variety of Mach numbers on configurations of practical interest. Additionally, the effectiveness of the transpiration method is demonstrated by its ability to model large scale continuous and discontinuous surface deflections without the computational expense of re-meshing at each CFD time-step.

Nomenclature

CFD	Computational Fluid Dynamics
M	Mach Number
ASE	Aeroservoelasticity
C_p	Pressure Coefficient
α	Angle of Attack (deg)
d	Control Surface Deflection (deg)
q	Generalized Displacement
F	Modal Displacement Matrix
η	Generalized Displacement Vector

Introduction

In the simulation of an aircraft's aeroelastic and aeroservoelastic characteristics, it is the time-marched CFD solution that requires the overwhelming proportion of CPU time. Dowell states that the computational time required is on the order of $P \times T_F$

* Graduate Research Assistant, Student Member AIAA

† Assistant Professor, Department of Mechanical and Aerospace Engineering, Senior Member AIAA.

‡ Aerospace Engineer, Member AIAA.

Copyright © 1998 by Cole H. Stephens. Published by the American Institute of Aeronautics and Astronautics, Inc. with permission.

where P is the number of parameter combinations required and T_F is the time required for a simultaneous fluid-structure time-marching calculation to complete a transient.¹ Even with continued improvements in flow algorithms and processor speeds, the computational demands generated by complicated three-dimensional configurations overwhelm the processors ability to develop a timely solution. These demands are further amplified when a modification of the existing computational grid is necessary. An expeditious ASE simulation is even more unrealizable when the entire computational grid must be modified at each CFD time-step to account for structural and/or control surface deflections.

An idea, first developed by Lighthill, has proven to be an effective tool for reducing the time required for unsteady aerodynamic calculations.² Lighthill used a method of equivalent sources to simulate changes in airfoil thickness. Instead of thickening the actual airfoil, an equivalent surface distribution of sources is used to *simulate* the boundary layer. This is done by modifying the normal velocity just outside the boundary layer to include additional outflow due to the boundary layer. The technique is also often used for boundary layer patching with inviscid flow techniques. Also more recently, the technique has been used to simulate surface deformations in full potential solution techniques, in addition to steady and unsteady rigid-body applications with Euler codes³⁻¹⁰.

Transpiration offers the advantage of being fast and relatively simple to implement. If, by some other means, the change in normal is known, then this change can be correlated to an appropriate change in surface normal on a CFD mesh and implemented directly on the existing grid.

An additional benefit of the transpiration method for boundary condition modeling is in aeroservoelastic problems. In such problems, it is often necessary to account for unsteady control surface deflections in the coupled CFD/Structural Dynamics simulation. These types of boundary conditions are problematic for unsteady CFD flow solvers due to the

very close proximity of control surface edges to adjacent parts of the airframe. Representing these adjacent surfaces in many cases would require contact between opposing surfaces of the mesh which is computationally intractable.

The objective of the current study is to investigate the use of the transpiration boundary condition approach when applied to steady and unsteady aeroelastic and aeroservoelastic problems using an Euler solver with unstructured meshes. Results for two different test cases address the extent to which the method may be used for geometries of practical interest.

Methodology

Computational analysis for the study was performed using the STARS codes developed at the NASA Dryden Flight Research Center¹¹. STARS is an highly integrated, finite-element based code for multidisciplinary analysis of flight vehicles including static and dynamic structural analysis, computational fluid dynamics, heat transfer, and aeroservoelasticity capabilities. All computations are performed on meshes consisting of unstructured tetrahedra.

In the present investigation, the transpiration boundary condition is utilized to simulate: static deformations, structural deformations during flutter, and control surface deflections. Structural calculations are performed using the finite element technique with modal superposition. Aeroelastic simulations are then performed through a coupling of a dynamics solver using the modal vectors, and the Euler aerodynamic solver. Additionally, static aeroelastic and control surface calculations were performed in which the simulated body deformation was compared with results obtained by deforming the actual structure and re-meshing the computational domain.

The actual surface deformations for the steady flow comparisons were accomplished by displacement of the surface tetrahedra through modal superposition¹⁴. Each surface node \mathbf{q}_{old} is displaced by the superposition of the nodal vectors each multiplied by a generalized displacement:

$$\mathbf{q}_{new} = \mathbf{q}_{old} + \Delta\mathbf{q}$$

where $\Delta\mathbf{q}(i)$ is determined by

$$\Delta\mathbf{q} = \Phi \mathbf{h}$$

where Φ is the modal displacement matrix and \mathbf{h} is the generalized displacement vector.

Control surface deflections are a result of a manual calculation of nodal displacements. For the transpiration study, the uniform change in normal due to a flap deflection is incorporated onto an existing CFD surface mesh. Constructing the actual deflected grid required knowledge of flap-wing intersection points and a total reconstruction of the CFD geometry.

Once the surface mesh has been deflected, the entire computational domain is re-meshed and the Euler solution is performed for comparison with the transpiration method.

The transpiration method is, quite simply, a means by which to *trick* the flow solver into seeing some sort of deflection in the mesh that is not actually there. If a change in surface normal is known, from a structural dynamics solver for example, then this change in normal could be applied directly to the existing CFD grid through a slight modification of the existing surface normals. The CFD solver has already calculated surface normals at each CFD node based on an average of the surrounding tetrahedra. With transpiration, the nodes affected by a surface deflection simply require a modification of its existing surface normal. Even though the surface is not actually deflected, all the flow solver sees is the normal at that particular nodal location, it does not matter what that normal is.

Results

Two representative test cases that have successfully implemented the transpiration boundary condition are presented. Test cases were chosen to highlight the effectiveness of the transpiration method even on relatively large surface deflections.

The first example is the AGARD wing. In this case, the transpiration boundary condition was used to couple the structural deformations from the dynamics solver to the Euler flow solver. Steady aeroelastic calculations were accomplished through arbitrary generalized displacements of all mode shapes. Unsteady aeroelastic simulations were performed through a coupling of the dynamics solver using the modal vectors and the Euler aerodynamics solver.

The second case is the BACT wing with a finite span flap. In this case, steady aerodynamic calculations are performed for a relatively large 10° flap deflection at transonic Mach numbers. Comparisons are made between solutions for the actual flap deflection and the simulated flap deflection using transpiration.

AGARD 445.6

The AGARD wing is a standard aeroelastic test configuration which has been investigated in the Langley Transonic Dynamics tunnel¹⁵. The wing has a 45° quarter chord sweep angle, aspect ratio of 1.65 and a taper ratio of 0.66. The airfoil cross-section is a NACA 65A004. Figure 1 is a planform view of the AGARD wing and the unstructured finite element CFD mesh generated in STARS.

Characteristic structural mode shapes were calculated using a structural dynamics routine in STARS on a *solids* mesh. These mode shapes included

first bending and first torsion. The superposition of these mode shapes provides the basis for the aeroelastic simulation. Application of the transpiration boundary condition on the surface of the wing allows the wing to dynamically deform at each intermediate CFD time step without modification to the surface or computational domain.

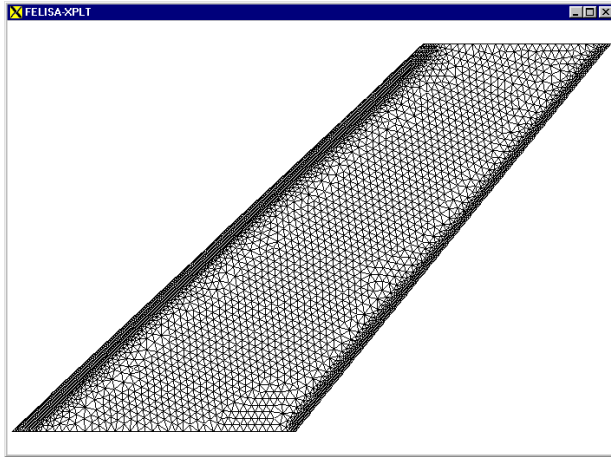


Figure 1: AGARD Test Wing Geometry and Surface Discretization

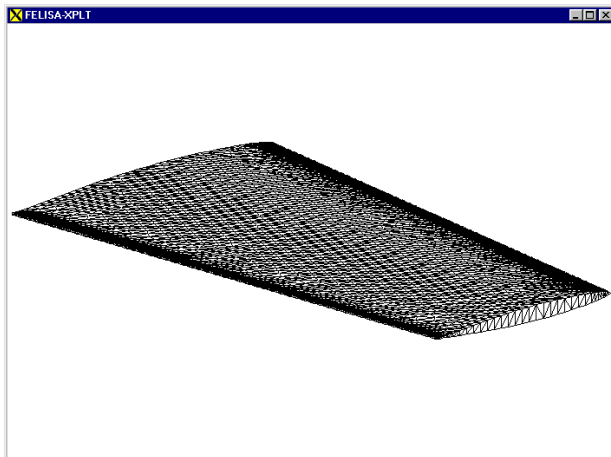


Figure 2: Transpiration Surface Mesh

Figure 2 and Figure 3 show the transpiration surface mesh and the corresponding deflected mesh. Transpiration was applied to the mesh in Figure 2 to simulate the actual deflection shown in Figure 3. The steady finite-element Euler flow solver in STARS is used to solve for the aerodynamic pressures for comparison of the actual and simulated structural deformation.

Figure 4 is an example of pressure contours on the surface of the AGARD wing. Along the span of the wing, sections marked A, B, and C show *cut-planes* along which pressure contours are plotted.

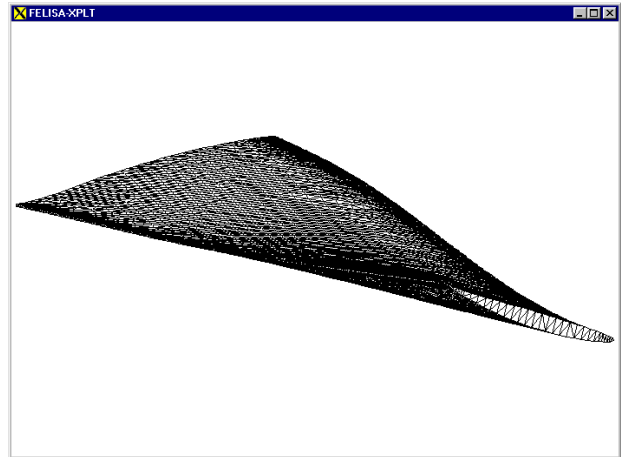


Figure 3: Deflected Surface Mesh

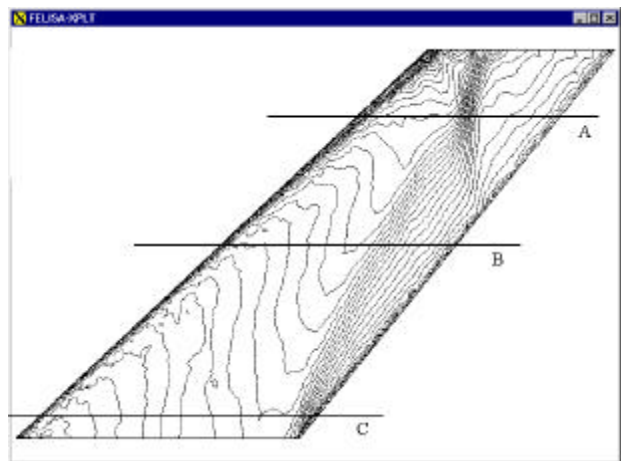


Figure 4: Pressure Contours at Mach 0.99

Figure 5, Figure 6, and Figure 7 are the resulting pressure distributions at *cuts* through the wing at locations indicated in Figure 4.

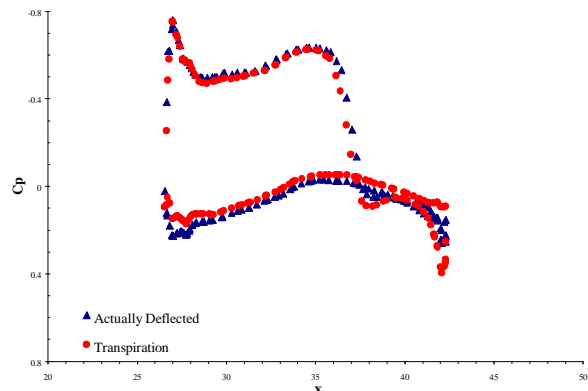


Figure 5: Pressure Distribution at Section A

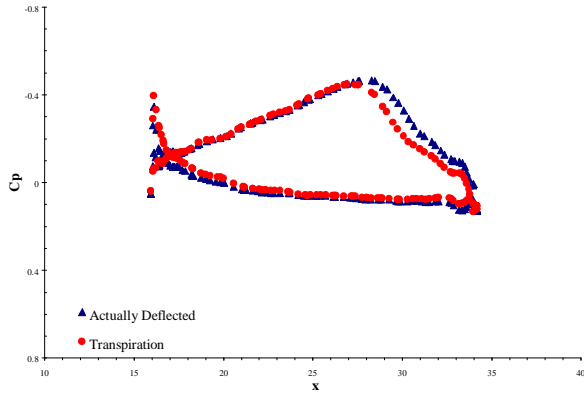


Figure 6: Pressure Distribution at Section B

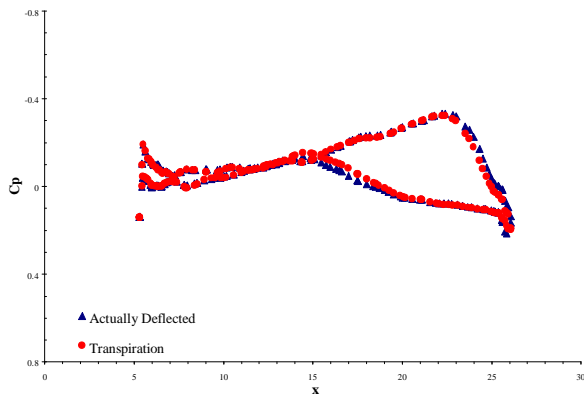


Figure 7: Pressure Distribution at Section C

Application of the transpiration method had little effect on the ability to predict flutter. Experimental flutter data was obtained at the Langley Transonic Dynamics tunnel and compared to flutter predictions using STARS. Figure 8 is a plot of flutter speed index vs. Mach number and illustrates STARS ability to predict flutter, even to the point of capturing the transonic dip.

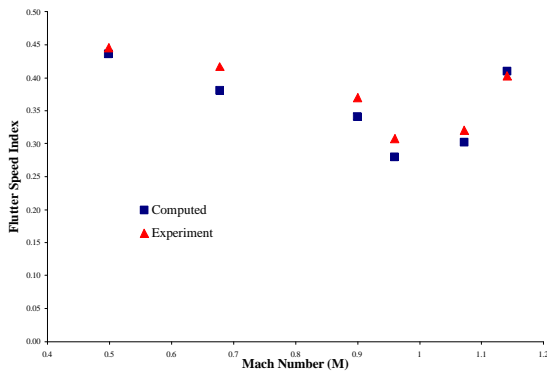


Figure 8: AGARD Wing Flutter Prediction and Comparison With Experiment

Results presented thus far highlight the effectiveness of the transpiration method when applied to larger scale, continuous structural deflections. Substantial difficulties arise when *discontinuous* structural deformations are to be modeled with contemporary mesh-deforming techniques. An obvious example is the deployment of a flap on a wing. Such deflections disrupt the continuity of the wing surface and introduce surfaces that are essentially non-existent when the control surface is in its stowed position. Modeling these narrow gaps between control surfaces and the opposite wing surfaces introduces a concentrated region in which the flow solution is adversely affected due to the scale of the gap in relation to the rest of the wing.

The following example investigates the efficacy of the transpiration method when applied to locally large, discontinuous surface deflections such as those experienced in the deflection of a control surface.

BACT Wing With 10° Flap Deflection

The BACT, Benchmark Active Controls Technology, wing is part of the Benchmark Models Program (BMP) at the NASA Langley Research Center¹³. The BMP program includes a series of models which were used to study different aeroelastic phenomena and to validate computational fluid dynamics codes.

The BACT wing has a rectangular planform with a NACA 0012 cross-section. The wings chord and span are 16 and 32 inches respectively. The trailing edge control surface is 25% of the chord, 30% of the total span of the wing, and is centered about the model 60% span station. Figure 9 shows a picture of the actual BACT wing used at Langley.

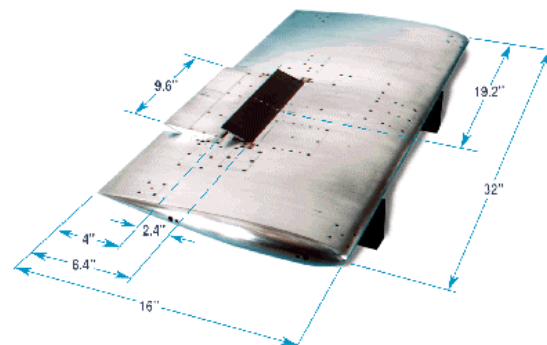


Figure 9: BACT Model

The wing also included 2 spoilers, one on the upper and lower surface of the wing in locations noted in Figure 9. For the present study, only the trailing edge control surface was modeled, the upper and lower spoilers were not.

Representative pressure plots were obtained at Mach numbers ranging from high-subsonic (Mach 0.77) and transonic (Mach 0.82) at an α of 0° . The 10° flap deflection was chosen to highlight the effectiveness of the transpiration method for large control surface deflections.

Figure 10 shows the surface mesh generated in STARS for the actual 10° flap deflection. Figure 11 shows an end-on view to more clearly show the extent of the flap deflection.

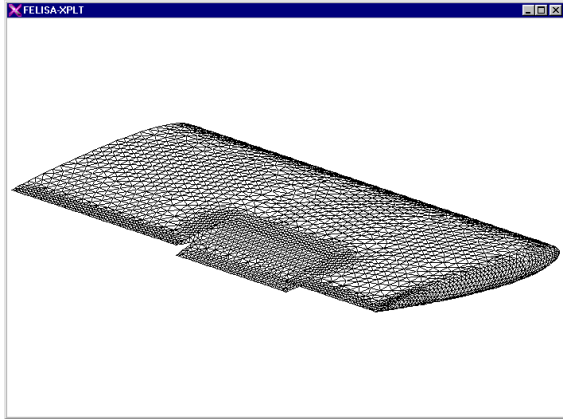


Figure 10: Surface Mesh for Actual 10° Flap Deflection



Figure 11: Profile of 10° Flap Deflection

The difficulty in modifying the mesh in Figure 10 is apparent when one looks at the varying intersection points along the control surface and the surface of the wing. Any slight modification in flap deflection angle requires that the entire geometry in the vicinity of the wing be re-calculated and re-meshed. This is, of course, time consuming.

Mesh deforming techniques are another means by which structural deflections are modeled. Deforming the mesh in an area where the surface goes from a smooth-continuous surface to a discontinuous surface leads to poor element structure. In the BACT case, however, the severe mesh shearing that would occur between the flap and the wing surfaces would lend itself to a poorly constructed mesh. Additionally, when a flap is deflected, there are *new* surfaces that would be exposed due to the displacement of the flap. The difficulty in modeling this sort of behavior is magnified with the desire of implementing a control algorithm to control aeroservoelastic flutter.

Transpiration is the most amiable alternative to re-defining the CFD surface mesh and resulting

computational grid. With transpiration, the flap deflection can be modified at each time step without having to modify the existing surface or computational domain. Shown in Figure 12 is an example of the type of mesh *shearing* that would have to take place within a moving mesh algorithm. In cases such as the BACT wing, the element stretching that occurs with mesh-deforming techniques would produce highly stretched, ill-conditioned tetrahedra in a place that actually should receive additional mesh refinement.

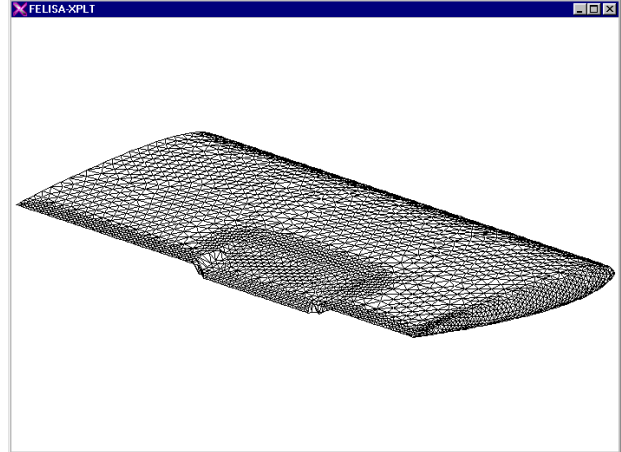


Figure 12: Mesh Shearing Example

With the transpiration method, all one needs to do is modify the generalized displacement by constant. Since there is no mesh modification necessary, the transition from one flap deflection angle to another is essentially instantaneous. Figure 13 and Figure 14 show the surface mesh used for the transpiration studies. Note that Figure 14 clearly shows that the transpiration mesh has no actual deflection.

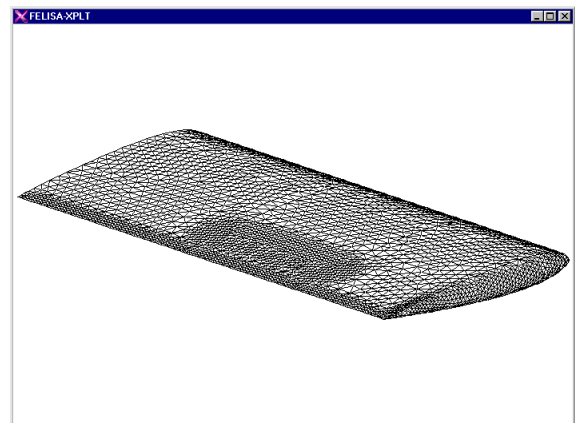


Figure 13: Surface Mesh for Simulated Flap Deflection

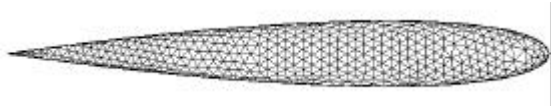


Figure 14: Profile of 10° Simulated Flap

The differences between the meshes for the actual and simulated flap deflections are kept at a minimum to eliminate any differences due to grid refinement.

Pressure contours on the surface of the wing are given in Figure 15 and Figure 16. These pressure contours are the result of the steady Euler solution at Mach 0.77, $\alpha=0^\circ$, and $\delta=10^\circ$. The difficulty in differentiating the two figures indicates the successful application of the transpiration boundary condition for a large surface deflection. Figure 15 shows the pressure contours for the case of an actual flap deflection. Figure 16 shows the pressure contours on the mesh in Figure 13 with a simulated flap deflection.

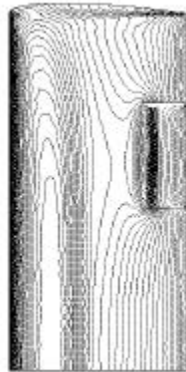


Figure 15: Surface Contours for 10° Flap Deflection at Mach 0.77 and $\alpha=0^\circ$

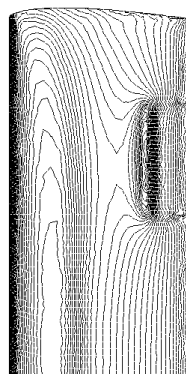


Figure 16: Surface Contours for 10° Simulated Flap Deflection at Mach 0.77 and $\alpha=0^\circ$

A qualitative comparison between Figure 15 and Figure 16 clearly shows the excellent agreement between the solutions. Slight differences exist but are not entirely due to the application of the transpiration boundary condition.

Convergence rates for these two cases were slightly different due to the difficulties associated with solutions in the transonic regime. Solutions appeared to be converging towards one-another, but are slightly different. Results have shown that extending the solution to exact agreement quickly reaches a point of diminishing returns.

Quantitative results are presented in the form of chord-wise pressure distributions at the wings 60% span. A chord-wise plane through this section corresponds to the mid-span of the flap. Figure 17 shows the superposition of the chord-wise pressure distributions.

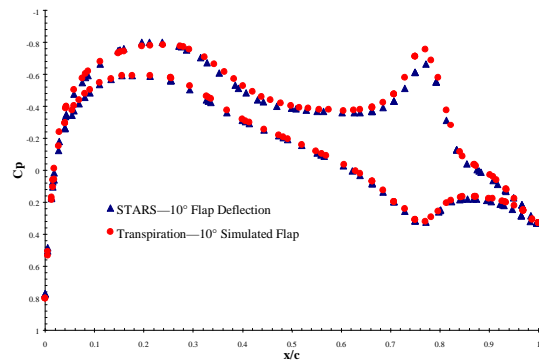


Figure 17: Actual and Simulated Flap Pressure Distributions at Mach 0.77, $\alpha=0^\circ$, and $\delta=10^\circ$

Except for the slight difference in peak C_p at the beginning of the flap, the actual and simulated flap show excellent agreement. Notice that Figure 17 does not clearly depict the existence of anything other than a weak transonic shock.

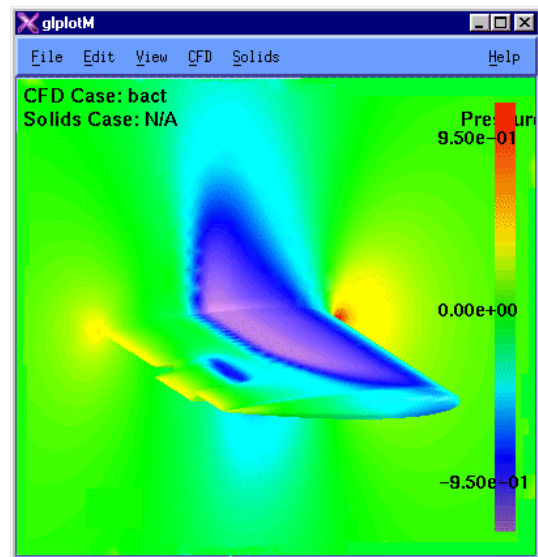


Figure 18: 3-D Pressure Contours at 0° α , Mach 0.82, 10° Flap Deflection

Another solution run at the same flap deflection and angle of attack, but at Mach 0.82 does have a very distinctive transonic shock.

Figure 18 and Figure 19 show a three-dimensional pressure distribution along the wing and the surrounding flow-field. This particular view allows the visualization of the complete three dimensional flow field and conveys a plethora of both qualitative and quantitative data. Again, excellent agreement is noted between the actually deflected mesh and the mesh modified through transpiration.

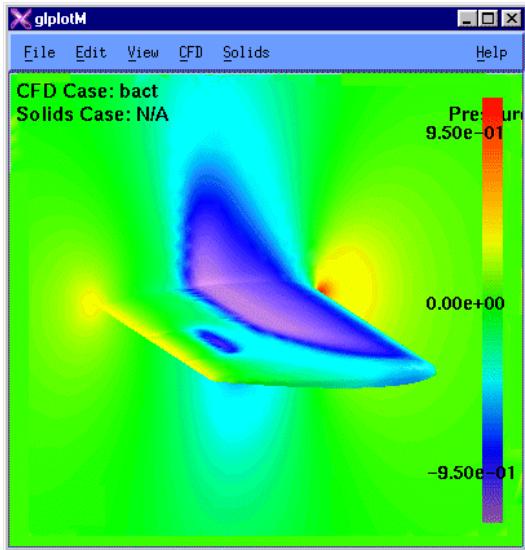


Figure 19: 3-D Pressure Contours at 0° α , Mach 0.82, 10° Simulated Flap Deflection

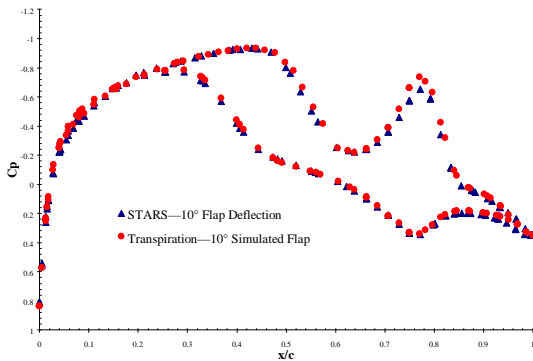


Figure 20: Actual and Simulated Flap Pressure Distributions at Mach 0.82, $\alpha=0^\circ$, and $c=10^\circ$

Figure 20 is again a superposition of chordwise pressure distributions at the mid-span of the flap. As was experienced with the Mach 0.77 case, the most significant difference was again at the beginning of the flap. Even with this large flap deflection, the transpiration method shows to be a viable tool in the analysis of control surface deflections for a varied range

of Mach numbers. As noted by Fisher and Arena, the reliability of the transpiration method was expected to diminish as the relative nodal displacements grew¹⁴. The BACT wing, with its relatively large flap deflection, expands the possible operating envelope for which the transpiration method is applicable.

Concluding Remarks

The purpose of the current study was to highlight the effectiveness of the transpiration method for aeroelastic and aeroservoelastic simulations in order to realize significant time savings. As has been shown, the transpiration method can be a valuable tool in coupled structural dynamics and CFD solutions where relatively large, continuous or discontinuous surface deformations are experienced.

The simplicity, ease of implementation, and versatility of the transpiration boundary condition make it an attractive, time-saving alternative to rediscretization or deforming mesh techniques.

Research in progress will use the transpiration method to simulate control surface deformations in a full unsteady aeroservoelastic simulation. Controlled deflection of a flap during aerodynamic flutter uses transpiration for control surface deflections as a means for flutter suppression.

Acknowledgements

Funds for the support of this study have been allocated through the NASA-Ames University Consortium Office, under Interchange Number NCC2-5105, and Oklahoma State University.

References

1. Dowell E.H., Crawley, E.F., Curtiss, Jr., H.C., Peters, D.A., Scanlan, R.H., and Sisto, F., "A Modern Course in Aeroelasticity", 3rd edition, Kluwer Academic Publishers, 1995.
2. Lighthill, M.J., "On Displacement Thickness," *Journal of Fluid Mechanics*, Vol. 4, Part 4, Jan. 1958, pp. 383-392.
3. Sankar, N.L., Malone, J.B., and Tassa, Y., "An Implicit Conservative Algorithm for Steady and Unsteady Three-Dimensional Transonic Potential Flows," AIAA Paper 81-1016, June 1981.
4. Malone, J.B., Sankar, L.N., and Sotomayer, W.A., "Unsteady Aerodynamic Modeling of a Fighter Wing in Transonic Flow," AIAA Paper 84-1566, AIAA 17th Fluid Dynamics, Plasma Dynamics, and Lasers Conference, Snowmass, CO, June 25-27, 1984.

5. Malone, J.B., and Sankar, L.N., "Unsteady Full Potential Calculations for Complex Wing-Body Configurations," AIAA Paper 85-4062.
6. Sankar, N.L., Ruo, S.Y., and Malone, J.B., "Application of Surface Transpiration in Computational Aerodynamics," AIAA Paper 86-0511, AIAA 24th Aerospace Sciences Meeting, Reno, NV, January 6-9, 1986.
7. Sankar, N.L., Malone, J.B., and Schuster, D., "Euler Solutions for Transonic Flow Past a Fighter Wing," *Journal of Aircraft*, Vol. 24, No. 1, Jan. 1987, pp. 10-16.
8. Ruo, S.Y., and Sankar, N.L., "Euler Calculations for Wing-Alone Configurations," *Journal of Aircraft*, Vol. 25, No. 5, May 1988, pp. 436-441.
9. Bharadvaj, Bala, K., "Computation of Steady and Unsteady Control Surface Loads in Transonic Flow," AIAA Paper 90-0935.
10. Raj, P. and Harris, B., "Using Surface Transpiration with an Euler Method for Cost-effective Aerodynamic Analysis," AIAA 93-3506, August, 1993.
11. Gupta, K.K., "STARS – An Integrated General-Purpose Finite Element Structural, Aeroelastic, and Aeroservoelastic Analysis Computer Program," NASA TM-4795, May, 1997.
12. Scott, R.C., Hoadley, S.T. Wiesman, C.D. and Durham, M.H., "The Benchmark Active Controls Technology Model Aerodynamic Data," AIAA Paper 97-0829, 35th Aerospace Sciences Meeting and Exhibit, Reno, NV, 1997.
13. Rivera, J.A., Jr., Dansberry, B.E., Bennett, R.M., Durham, M.H., and Silva, W.A., "NACA 0012 Benchmark Model Experimental Flutter Results With Unsteady Pressure Distributions. NASA TM-107581, March 1992.
14. Fisher, C.F., and Arena, Jr., A.S., "On the Transpiration Method for Efficient Aeroelastic Analysis Using an Euler Solver," AIAA 96-3436, August 1996.
15. Yates, E.C., Jr., Land, N.S., and Foughner, J.T., Jr., "Measured and Calculated Subsonic and Transonic Flutter Characteristics of a 45° Sweptback Wing Planform in Air and Freon-12 in the Langley Transonic Dynamics Tunnel," NASA TN D-1616, March 1963.
16. Arena, Jr., A.S., Voelker, L.S. and Gupta, K.K., "Applications of Time-Marched Finite Element Euler Solutions for Aeroelastic Prediction," 10th International Conference on Finite Elements in Fluids, Tucson, AZ, January 5-8, 1998.